Computational Materials Science 58 (2012) 227–235

Contents lists available at SciVerse ScienceDirect

Computational Materials Science

journal homepage: www.elsevier.com/locate/commatsci

AFLOWLIB.ORG: A distributed materials properties repository from high-throughput *ab initio* calculations

Stefano Curtarolo [a,b,c,*], Wahyu Setyawan [a,1], Shidong Wang [a], Junkai Xue [a], Kesong Yang [a], Richard H. Taylor [a], Lance J. Nelson [d], Gus L.W. Hart [d], Stefano Sanvito [e], Marco Buongiorno-Nardelli [f,c], Natalio Mingo [g], Ohad Levy [h]

[a] Department of Mechanical Engineering and Materials Science, Duke University, Durham, NC 27708, United States
[b] Department of Physics, Duke University, Durham, NC 27708, United States
[c] Computer Science and Mathematics Division, Oak Ridge National Laboratory, Oak Ridge, TN 37831, United States
[d] Department of Physics and Astronomy, Brigham Young University, Provo, UT 84602, United States
[e] School of Physics and CRANN, Trinity College, Dublin 2, Ireland
[f] Department of Physics, University of North Texas, Denton, TX 76203, United States
[g] LITEN, CEA-Grenoble, 17 rue des Martyrs, 38054 Grenoble Cedex 9, France
[h] Department of Physics, NRCN, P.O. Box 9001, Beer-Sheva 84190, Israel

ARTICLE INFO

Article history:
Received 15 November 2011
Accepted 1 February 2012

Keywords:
High-throughput
Combinatorial materials science
Ab initio
AFLOW
Materials genome initiative

ABSTRACT

Empirical databases of crystal structures and thermodynamic properties are fundamental tools for materials research. Recent rapid proliferation of computational data on materials properties presents the possibility to complement and extend the databases where the experimental data is lacking or difficult to obtain. Enhanced repositories that integrate both computational and empirical approaches open novel opportunities for structure discovery and optimization, including uncovering of unsuspected compounds, metastable structures and correlations between various characteristics. The practical realization of these opportunities depends on a systematic compilation and classification of the generated data in addition to an accessible interface for the materials science community. In this paper we present an extensive repository, aflowlib.org, comprising phase-diagrams, electronic structure and magnetic properties, generated by the high-throughput framework AFLOW. This continuously updated compilation currently contains over 150,000 thermodynamic entries for alloys, covering the entire composition range of more than 650 binary systems, 13,000 electronic structure analyses of inorganic compounds, and 50,000 entries for novel potential magnetic and spintronics systems. The repository is available for the scientific community on the website of the materials research consortium, aflowlib.org.

1. Introduction

The development of new materials is a difficult enterprise because of the vast number of possible combinations of elements and crystal structures. In developing a new material, or improving one already in use, the materials scientist usually relies on the huge body of empirical information on crystal structures and materials properties compiled into various databases. Among the most widely used databases of inorganic materials are those of metals, intermetallics and minerals crystal structures: CRYSTMET [1], ICSD [2], Pearson's Crystal Data [3], Pauling File Inorganic Materials Database [4]), and binary alloy phase diagrams [5,6]. These empirical databases are understandably incomplete, not only due to the vast combination space (most of which has not been explored [7]), but also since experimentation in many cases is difficult, requiring high temperatures and/or pressures, very long equilibration processes, or materials that are hazardous, highly reactive, poisonous or radioactive. Computational compilation of materials properties is more feasible, and will lead to much more complete repositories.

The dramatic advances made over the last half century in calculating material properties quickly and accurately, based on quantum-mechanical approaches, have spawned the new discipline of computational materials science. They make it possible to create computationally-derived repositories, that significantly complement existing empirical data, and use them for rational material

* Corresponding author at: Department of Mechanical Engineering and Materials Science, Duke University, Durham, NC 27708, United States. Tel.: +1 919 660 5506; fax: +1 919 660 8963.
E-mail address: stefano@duke.edu (S. Curtarolo).
[1] Present address: Pacific Northwest National Laboratory, Richland, WA 99354, United States.

0927-0256/$ - see front matter © 2012 Elsevier B.V. All rights reserved.
doi:10.1016/j.commatsci.2012.02.002

design. Generating such repositories requires efficient screening of large sets of structures with many different combinations of elements and compositions in a *high-throughput* (HT) fashion.

In this paper we describe aflowlib.org, a library of databases of material properties generated using the HT framework AFLOW [8], that may be mined *a posteriori* for various, *a priori* unanticipated, applications. It currently includes repositories of

i. phase-diagrams, free energies, stable and metastable structures of binary alloy systems (*Binary Alloy Project*, Section 2),
ii. electronic structure of inorganic compounds (*Electronic Structure Database*, Section 3) and
iii. electronic and magnetic properties of alloys (*Magnetic Database*, Section 5).

The databases are undergoing continuous development and extension. They are accessible on our website, aflowlib.org.

Other online materials initiatives include the Materials Project, (materialsproject.org) [9], and the Computational Materials Repository, (wiki.fysik.dtu.dk/cmr).

2. The binary alloy project

An extensive database of binary phase-diagrams, compounds, and metastable structures (the "binary alloy library" project) was created by using the AFLOW framework [8]. The generation of the library required several tens of millions of cpu hours. It currently contains over 150,000 alloy entries spanning the entire composition range of more than 650 binary systems of the transition metals, alkaline earths and alkali metals. Each entry includes the groundstate energy and magnetic moment per atom, the crystal structure space group and prototype or the *Strukturbericht* designation. This alloy database is updated regularly and extended periodically. It may be accessed online at aflowlib.org through the user interface shown in Fig. 1.

The interface allows the user to review the following options for each of the binary systems included in the repository:

- all; The complete list of structures calculated for the specified system. The original and relaxed structure data (including unit cell vectors, atom coordinates, calculated energy, magnetic

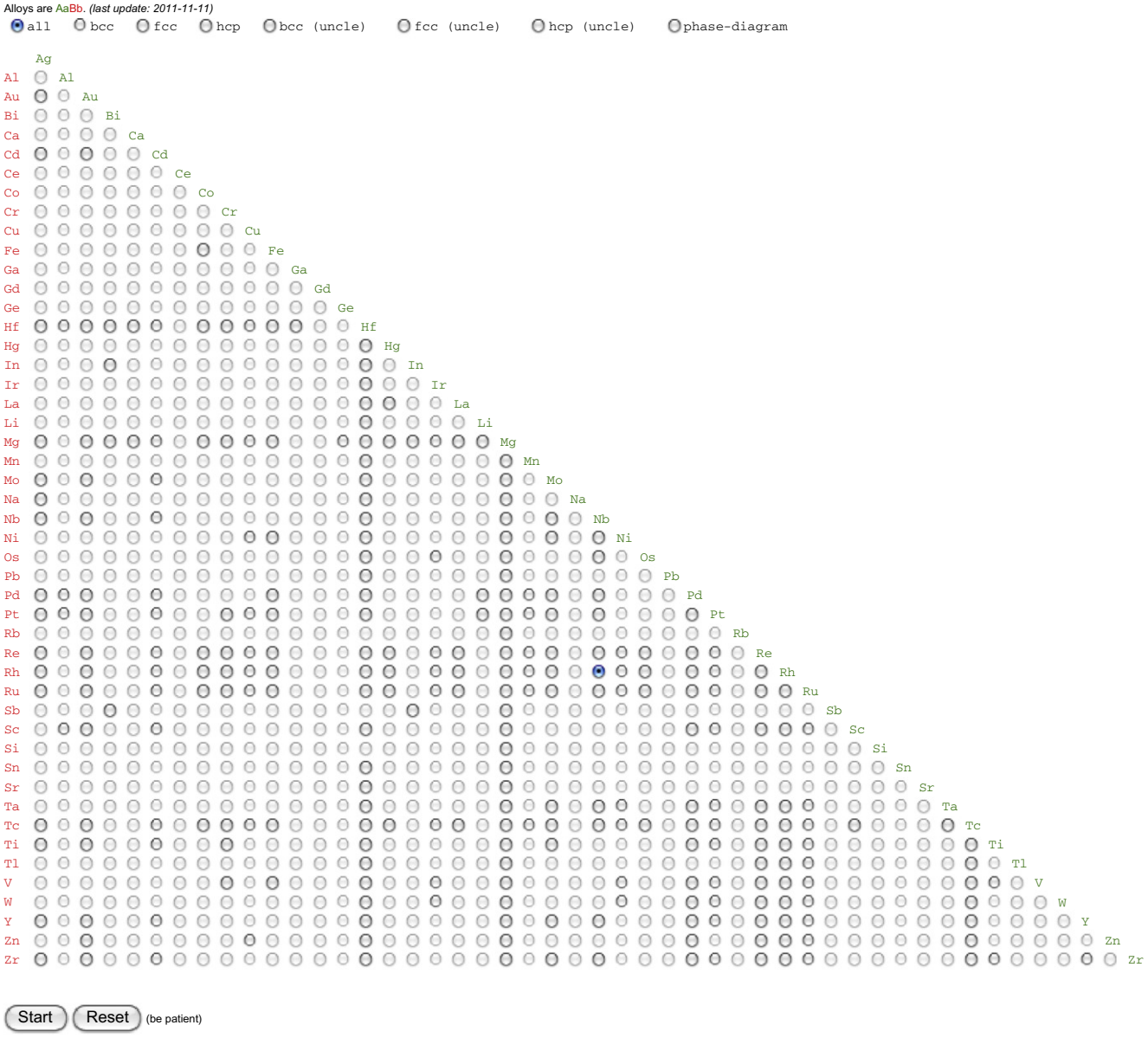

Fig. 1. Input interface of the aflowlib.org alloy library of binary systems.

moment and volume per atom) is provided for each entry, as shown in Fig. 2. Fig. 3 is an example of a list of equiatomic structures calculated for the Nb–Rh binary system, where $L1_0$ is identified as a ground-state of the system (labeled by `Emin-GND`). It demonstrates the ability of AFLOW to identify relaxation of structures into others, e.g., the second structure listed in Fig. 3 starts as prototype B10 (space group #129) but relaxes into $L1_0$ (space group #123).

- bcc, fcc or hcp; lists of bcc-, fcc- or hcp-based structures calculated for the selected system, respectively. These lattice specific lists are useful for implementing cluster expansion calculations [10].
- phase diagram; the zero-temperature phase diagram of the selected binary system. For each structure in the database, the formation enthalpy was calculated from the lowest-energy elemental form of the constituents. AFLOW automatically constructs the convex hull, from the structures of extremal energy at the various concentrations, and generates the phase diagram as shown in Fig. 4.

This database of binary alloys has been used in several studies to identify hitherto unknown stable phases in several alloy classes. In one case, 34 Mg binary systems were examined [11]. In about one third of the systems, the *ab initio* results identified all the known experimental phases and predicted additional stable phases. Moreover, seven systems Mg–Na, Mg–Tc, Mg–Zr, Ir–Mg, Mg–Pb, Mg–Pd, and Mg–Rh, thought to be non-compound-forming based on experimental evidence were predicted to have stable phases. This new thermodynamic information may be useful for the development of improved lightweight alloys.

High-throughput studies were also undertaken for several platinum group metals, Rh, Re, and Ru [12–14]. These metals are of particular interest because of their many applications as catalytic materials. The picture of these alloys that emerges from the extensive calculated database is considerably different from that depicted by experimental data. Many of the ostensibly phase-separating systems are predicted to have stable structures. Although some of the predicted phases may only be stable at temperatures where sluggish kinetics inhibits their formation, they serve as a guide to further experimental studies, usefully narrowing the field of compositions to be attempted. Furthermore, even if the bulk phases might not exist at room temperature, ordered structures might be stable at the nano-scale, e.g. for a few nano-catalysts (Fe–C, Fe–Mo–C, Pt), it was shown that the surface-tension contribution to the free energy plays a fundamental role in stabilizing ordered structures, thereby causing catalytic deactivation [15–17]. Thus, to design effective catalytic nano-systems it is necessary to be aware of all the possible competing phases, even if they are not kinetically accessible in the bulk.

The ground state predictions of binary alloy crystal structures generated in these high-throughput *ab initio* studies have been found to be highly accurate. It was shown that the probability of reproducing the correct ground state, if well defined and not ambiguous, is ~96.7% (reliability of the method, Eq. (3) in Ref. [18]). Extensive studies of hafnium-based alloys [19], techne-

```
# ------------------------------------------------------------
NbRh/292
# Structure PRE ------------------------------------------------
Nb_svRh_pv.292
-66.076200
   3.99980000000000   0.00000000000000   0.00000000000000
   0.00000000000000   3.99980000000000   0.00000000000000
   0.00000000000000   0.00000000000000   5.06540000000000
2 2  Direct(4) [A2B2]
   0.25000000000000   0.25000000000000   0.23420000000000  Nb
   0.75000000000000   0.75000000000000   0.76580000000000  Nb
   0.25000000000000   0.75000000000000   0.00000000000000  Rh
   0.75000000000000   0.25000000000000   0.00000000000000  Rh
# Structure POST -----------------------------------------------
Nb_svRh_pv.292
0.934225
   4.32163818537409   0.00000000000000   0.00000000000000
   0.00000000000000   4.32163818537409  -0.00000000000000
   0.00000000000000   0.00000000000000   4.15998906360566
2 2  Direct(4) [A2B2]
   0.25000000000000   0.25000000000000   0.49523191611840  Nb
   0.75000000000000   0.75000000000000   0.50476808388160  Nb
   0.25000000000000   0.75000000000000   0.00000000000000  Rh
   0.75000000000000   0.25000000000000   0.00000000000000  Rh
# ------------------------------------------------------------
 -0.43378830000000   # Ef/at (VASP)
  0.00000000000000   # Mom/at
 15.83740000000000   # Volume/at
  0.50000000000000   # Ca
  0.50000000000000   # Cb
     P4/nmm #129     # space group PRE
     P4/mmm #123     # space group POST  XX
# ------------------------------------------------------------
```

Fig. 2. Structure data example, pre- and post-relaxation, including the AFLOW structure label, unit cell vectors, composition and atom coordinates. In this example NbRh-B10 relaxes to $L1_0$.

```
CONCENTRATION=0.5000000
 *str=   3 Ef=-0.4358 dEf=0.0000 sg=[ P4/mmm #123| P4/mmm #123]   L1_0 AuCu (0.0) Emin-GND
  str= 292 Ef=-0.4338 dEf=0.0020 sg=[ P4/nmm #129| P4/mmm #123]XX B10 PbO/PbS (0.0)
 *str=  60 Ef=-0.4332 dEf=0.0027 sg=[    Cmmm #65| P4/mmm #123]XX \gamma-IrV (0.0)
  str=  74 Ef=-0.4278 dEf=0.0080 sg=[   P21/m #11|   P21/m #11]   74 (0.0)
  str= 120 Ef=-0.4130 dEf=0.0228 sg=[    Pmma #51|    Pmma #51]   B19 AuCd (0.0)
  str= 192 Ef=-0.4021 dEf=0.0338 sg=[    Cmcm #63|    Cmcm #63]   B33 CrB (0.0)
  str= 256 Ef=-0.3976 dEf=0.0382 sg=[    Pnma #62|    Pnma #62]   B27 BFe (0.0)
  str=  17 Ef=-0.3632 dEf=0.0726 sg=[    C2/m #12|    C2/m #12]   W2 FCC_{A2B2}^{[311]} (0.0)
  str=  77 Ef=-0.3459 dEf=0.0899 sg=[ P4/nmm #129| P4/nmm #129]   B11 \gamma-CuTi BCC_{A2B2}^{[001]} (0.0)
  str=  20 Ef=-0.3446 dEf=0.0912 sg=[    Pmmn #59|    Pmmn #59]   M(AgZr) Y2 FCC_{A2B2}^{[011]} (0.0)
  str=  23 Ef=-0.3321 dEf=0.1037 sg=[I41/amd #141|I41/amd #141]   CH 40 NbAs/NbP (0.0)
  str=  80 Ef=-0.3315 dEf=0.1043 sg=[    Imma #74|I41/amd #141]XX 80 (0.0)
  str= 138 Ef=-0.3238 dEf=0.1120 sg=[       Cm #8|       Cm #8]   138 (0.0)
  str= 291 Ef=-0.3084 dEf=0.1274 sg=[ P4/nmm #129| P4/nmm #129]   B10 PbO/PbS (0.0)
  str= 123 Ef=-0.3047 dEf=0.1311 sg=[    C2/m #12|    C2/m #12]   123 (0.0)
  str= 139 Ef=-0.2870 dEf=0.1488 sg=[       Cm #8|       Cm #8]   139 (0.0)
  str= 195 Ef=-0.2558 dEf=0.1800 sg=[   P213 #198|   P213 #198]   B20 FeSi (0.0)
  str= 136 Ef=-0.2491 dEf=0.1867 sg=[       Cm #8|       Cm #8]   136 (0.0)
  str=  85 Ef=-0.2471 dEf=0.1887 sg=[  Fd-3m #227|  Fd-3m #227]   B32 NaTl (0.0)
  str= 119 Ef=-0.2409 dEf=0.1950 sg=[    Pmmn #59|    Pmmn #59]   oP4 CuTe (0.0)
  str= 116 Ef=-0.2383 dEf=0.1975 sg=[  P-6m2 #187|  P-6m2 #187]   B_h WC (0.0)
  str= 193 Ef=-0.2354 dEf=0.2004 sg=[    Cmcm #63|    Cmcm #63]   B33 CrB (0.0)
  str= 194 Ef=-0.2343 dEf=0.2015 sg=[    Cmcm #63|    Cmcm #63]   TlI (0.0)
  str=  61 Ef=-0.1992 dEf=0.2366 sg=[  Pm-3m #221|  Pm-3m #221]   B2 CsCl (0.0)
  str=   4 Ef=-0.1929 dEf=0.2429 sg=[   R-3m #166|   R-3m #166]   L1_1 CuPt (0.0)
  str= 220 Ef=-0.1753 dEf=0.2605 sg=[P63/mmc #194|P63/mmc #194]   B8_1 NiAs (0.0)
  str=  71 Ef=-0.1565 dEf=0.2793 sg=[    Cmma #67|    Cmma #67]   71 (0.0)
  str= 196 Ef=-0.1388 dEf=0.2970 sg=[ P4/nmm #129| P4/nmm #129]   CdTi (0.0)
  str= 197 Ef=-0.1386 dEf=0.2972 sg=[ P4/nmm #129| P4/nmm #129]   CdTi (0.0)
  str=  14 Ef=-0.1366 dEf=0.2993 sg=[ P4/nmm #129| P4/nmm #129]   Z2 FCC_{A2B2}^{[001]} (0.0)
  str= 126 Ef=-0.1318 dEf=0.3040 sg=[  P-3m1 #164|  P-3m1 #164]   126 (0.0)
  str=  28 Ef=-0.0909 dEf=0.3449 sg=[   R-3m #166|   R-3m #166]   V2 FCC_{A2B2}^{[111]} (0.0)
  str= 221 Ef=-0.0690 dEf=0.3668 sg=[P63/mmc #194|P63/mmc #194]   B8_1 NiAs (0.0)
  str= 407 Ef=+0.0046 dEf=0.4404 sg=[P63/mmc #194|P63/mmc #194]   LiB-MS2 (0.0)
  str= 201 Ef=+0.0980 dEf=0.5338 sg=[  Fm-3m #225|  Fm-3m #225]   B1 NaCl (0.0)
  str= 219 Ef=+0.7047 dEf=1.1405 sg=[  P63mc #186|  P63mc #186]   B4 ZnS Wurtzite (0.0)
  str= 218 Ef=+0.7166 dEf=1.1524 sg=[  F-43m #216|  F-43m #216]   B3 ZnS zincblende (0.0)
```

Fig. 3. Example of a structure list, showing NbRh equiatomic structures calculated by AFLOW.

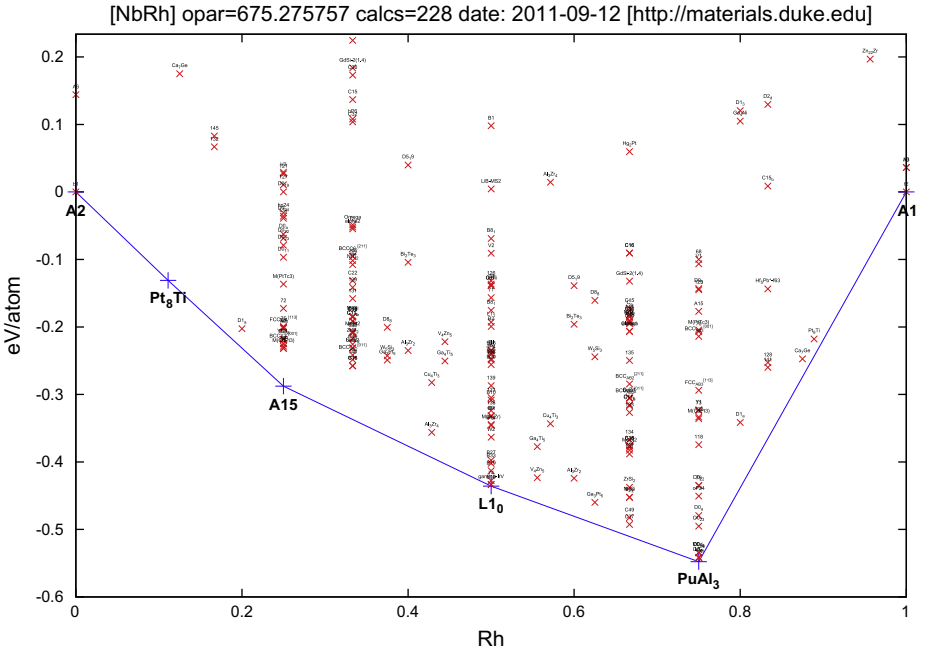

Fig. 4. Example of a binary phase diagram, Nb–Rh, generated automatically by AFLOW from groundstate energies of over 220 crystal structures.

tium-based alloys [20], as well as hcp-based intermetallic alloys [21], demonstrated how high-throughput studies can be coupled with other computational techniques, e.g. cluster expansion, or with empirical data, e.g. Pettifor maps, to yield a more complete picture of alloy thermodynamics where experiments are incomplete or difficult to carry on.

3. The electronic structure database

The long term purpose of this repository is to provide the community with electronic structure data on all the known experimental compounds. This formidable task is still in progress. In the first stage we are considering the compounds included in the ICSD database [22]. Of the 200,000+ entries available in the ICSD, 13,000 have already been calculated. We use the AFLOW materials framework within the DFT+U formalism, as explained in Ref. [8]. The data on the calculated structures is available on the aflowlib.org website for rapid searching by online users. Fig. 5 shows the current electronic structure database interface.

The user may specify the following options and perform the requested search through the ''Submit Query'' button.

- Choose Databases. The user can choose the properties to be searched by selecting *Structure* [8], *Electronic* [25], *Thermoelectric* [24], *Scintillator* [23], and *Magnetic* properties. The last option, *"Job Status"*, is reserved for development purposes.
- Name or ICSD Number. Specify the composition of the compound in alphabetic order (e.g., O1Zn1, Al2O3) or the ICSD number (e.g., 82,504, 9770). If there are available entries, they will appear in the results screen.
- Element(s). Specify a combination of elements, using the keywords &(and), |(or), ~(not), ∧(xor), and a label *m*(metals) indicating all the metals. For instance, the user can specify "Ag & m & ~Cd" to obtain all the multi-component compounds containing silver, another metal except cadmium, and any other element.
- Species Number. In this field the user can specify the number of components in the search. For instance, if the previous search, "Ag & m & ~Cd", results in 3-, 4-, 5- and 6-components entries, the user can limit it to quaternary systems by specifying 4 in this field.
- Material Type. In this field the user can choose to limit the search to *metals* or *semiconductors/insulators*.
- Lattice System. Restrict the results to one of the seven lattice systems: *cubic, hexagonal, rhombohedral, tetragonal, orthorhombic, monoclinic, triclinic*
- Bravais Lattice. Restrict the results to one of the 14 Bravais Lattices: *cub, fcc, bcc, hex, rhl, tet, bct, orc, orcc, orcf, orci, mcl, mclc, tri* [25].
- Space Group Number. Restrict the search to structures with one of the 230 space groups.
- Pearson Symbol. Specify a particular Pearson symbol.
- Minimum/Maximum Band Gap. In these two fields the user can search for materials with the band gap within certain limits [23].
- *n*- or *p*-type Power Factor.
- Minimum/Maximum Magnetic Moment. Search for materials with magnetic moment/per atom within the specified limits.
- Minimum/Maximum $\Delta S(E_f)$. Search for materials with up/down spin difference at the Fermi energy within the specified limits.
- Aflow Version from/to and Calculation Date from/to. These options are used to debug the AFLOW code.
- Results per page. The number of entries presented on each page of results.

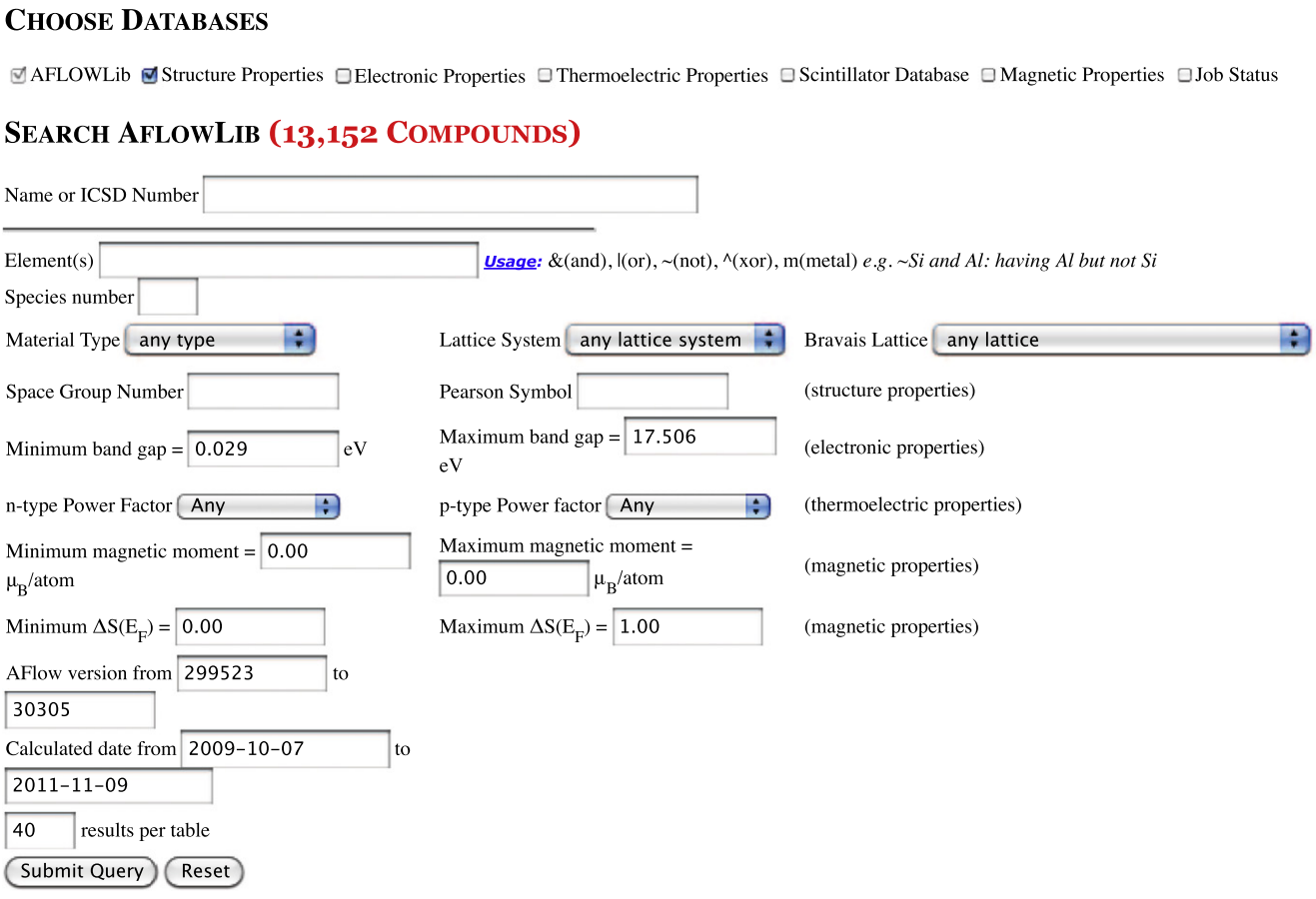

Fig. 5. The input interface for the crystallographic, electronic structure, thermoelectric and magnetic database of aflowlib.org.

Typical results of searches are shown in Figs. 6–9.

Fig. 10 shows an example of an entry in this database, $Al_1Ca_1O_5Ta_1$ (ICSD #99001). The page includes:

- Permanent URL. The permanent link of the compound on aflowlib.org. By pointing to this unique URL, the user will always find this compound independently of the actual position of the entry in the servers of the consortium.
- Relaxed Real Space Lattice. *Ab initio* relaxed geometry (a, b, c, α, β, γ,), volume, number of atoms per cell and density of the compound.
- Bravais Lattice of the Crystal. Space group, Pearson Symbol, Bravais Lattice of the primitive cell, variation of the Bravais Lattice [25], and Bravais system for the crystal, where all the basis atoms of the cell are considered. This is the information used to generate the Brillouin Zone [25]. Within AFLOW this information is extracted by the option –pgroup_xtal.

Index	▲Name [1]	ICSD Number [1]	Bravais Lattice	Number of Atoms	Space Group Number	Pearson Symbol	Density (g/cm^3)	Proto Name
1	$Ag_1Fe_1O_2$	2786	HEX (Hexagonal)	8	194 (P63/mmc)	hP8	6.55	Ag1Fe1O2_ICSD_2786
2	$Ag_1Fe_1O_2$	31919	RHL (Rhombohedral)	4	166 (R-3mH)	hR4	6.55	Ag1Fe1O2_ICSD_31919
3	$Ag_2Fe_1S_4Sn_1$	42534	BCT (Tetragonal)	8	121 (I-42m)	tI16	4.77	Ag2Fe1S4Sn1_ICSD_42534

Fig. 6. Results of a *Structure Properties* search within aflowlib.org. From left to right: index, compound name, ICSD number, Bravais Lattice, Number of Atoms per Cell, Space Group number, Pearson Symbol, Density (gr/cm^3), Prototype Name.

Index	▲Name [1]	ICSD Number [1]	Bravais Lattice	Number of Atoms	Band Gap (eV) [2,3]	Fit Band Gap (eV) [2,3]	m_e (m_0) [2,3]	m_e^{min} (m_0) [2,3]	m_h (m_0) [2,3]	m_h^{min} (m_0) [2,3]	Mass ratio [3]	Valence Band Width (eV) [3]	Core Valence Gap (eV) [3]	Attenuation Length (cm) [3]	Proto Name
1	$Ca_1Fe_3O_{12}Ti_4$	79277	BCC (Cubic)	20	2.00 (D)	3.62	0.98	0.97	2.93	1.79	2.99	6.11	10.61	2.56100	Ca1Fe3O12Ti4_ICSD_79277
2	Cl_2Fe_1	64831	HEX (Hexagonal)	3	3.21 (I)	5.24	21.90	1.48	8.23	3.54	2.66	5.25	8.40	3.68000	Cl2Fe1_ICSD_64831
3	F_2Fe_1	9166	TET (Tetragonal)	6	2.63 (I)	4.46	0.49	0.48	190.80	5.47	388.39	7.15	15.23	2.86700	F2Fe1_ICSD_9166

Fig. 7. Results of a *Electronic* and *Scintillator Properties* search within aflowlib.org. From left to right: index, name, ICSD number, Bravais Lattice, Number of Atoms per Cell, Band Gap (eV), Fitted Band Gap (eV), effective mass of the electrons near the conduction band m_e, effective mass of the electrons at the minimum of the conduction band m_e^{min}, effective mass of the holes near the valence band m_h, effective mass of the holes at the minimum of the valence band m_e^{min}, mismatch mass ratio $m_r = min(m_e/m_h, m_h/m_e)$, Valence Band Width (eV), Core Valence Gap (eV), Attenuation Length (cm), Prototype Name. For definitions see Ref. [23].

Index	▲Name [1]	ICSD Number [1]	Bravais Lattice	Number of Atoms	<P_n>/L (μW/cmK²nm) [4]	<P_{n1}>/L (μW/cmK²nm) [4]	<P_{n2}>/L (μW/cmK²nm) [4]	<P_{n3}>/L (μW/cmK²nm) [4]	<P_p>/L (μW/cmK²nm) [4]	<P_{p1}>/L (μW/cmK²nm) [4]	<P_{p2}>/L (μW/cmK²nm) [4]	<P_{p3}>/L (μW/cmK²nm) [4]	S_n (μV/K) [4]	S_p (μV/K) [4]	Prototype Name
1	$F_3Fe_1K_1$	15424	CUB (Cubic)	5	0.15	0.15	0.15	0.15	2.17	2.17	2.17	2.17	-116.36	91.29	F3Fe1K1_ICSD_15424
2	$F_3Fe_1Rb_1$	49586	CUB (Cubic)	5	0.24	0.24	0.24	0.24	1.50	1.48	1.51	1.51	-91.73	91.04	F3Fe1Rb1_ICSD_49586
3	$Fe_1La_1O_3$	29118	CUB (Cubic)	5	0.31	0.31	0.31	0.31	2.00	2.00	2.00	2.00	-139.02	92.92	Fe1La1O3_ICSD_29118

Fig. 8. Results of a *Thermoelectric Properties* search within aflowlib.org. From left to right: index, name, ICSD number, Bravais Lattice, Number of Atoms, Relative Power Factors $\langle P \rangle / L$ of n- and p-doped nano-sintered compounds (average and projections over x, y, z), Seebeck coefficients for n- and p-doped cases (μ V/K), Prototype Name. For definitions see Ref. [24].

Index	▲Name [1]	ICSD Number [1]	Bravais Lattice	Number of Atoms	Magnetic Moment (μ_B/atom) [5]	Spin Polarization (1/atom) [5]	Spin Decomposition (μ_B)	Prototype Name
1	$Ag_1Fe_1O_2$	2786	HEX (Hexagonal)	8	1.25	0.00	{0.039,0.039,4.303,4.303,0.258,0.258,0.258,0.258}	Ag1Fe1O2_ICSD_2786
2	$Ag_1Fe_1O_2$	31919	RHL (Rhombohedral)	4	1.25	0.00	{0.039,4.303,0.258,0.258}	Ag1Fe1O2_ICSD_31919
3	$Ag_2Fe_1S_4Sn_1$	42534	BCT (Tetragonal)	8	0.50	0.00	{0.016,0.016,3.631,0.024,0.024,0.024,0.024,0.016}	Ag2Fe1S4Sn1_ICSD_42534

Fig. 9. Results of a *Magnetic Properties* search within aflowlib.org. From left to right: index, name, ICSD #, Bravais Lattice, Number of Atoms, Magnetic Moment (μ_B/atom), Spin Polarization per atom, Spin Decomposition (μ_B), Prototype Name.

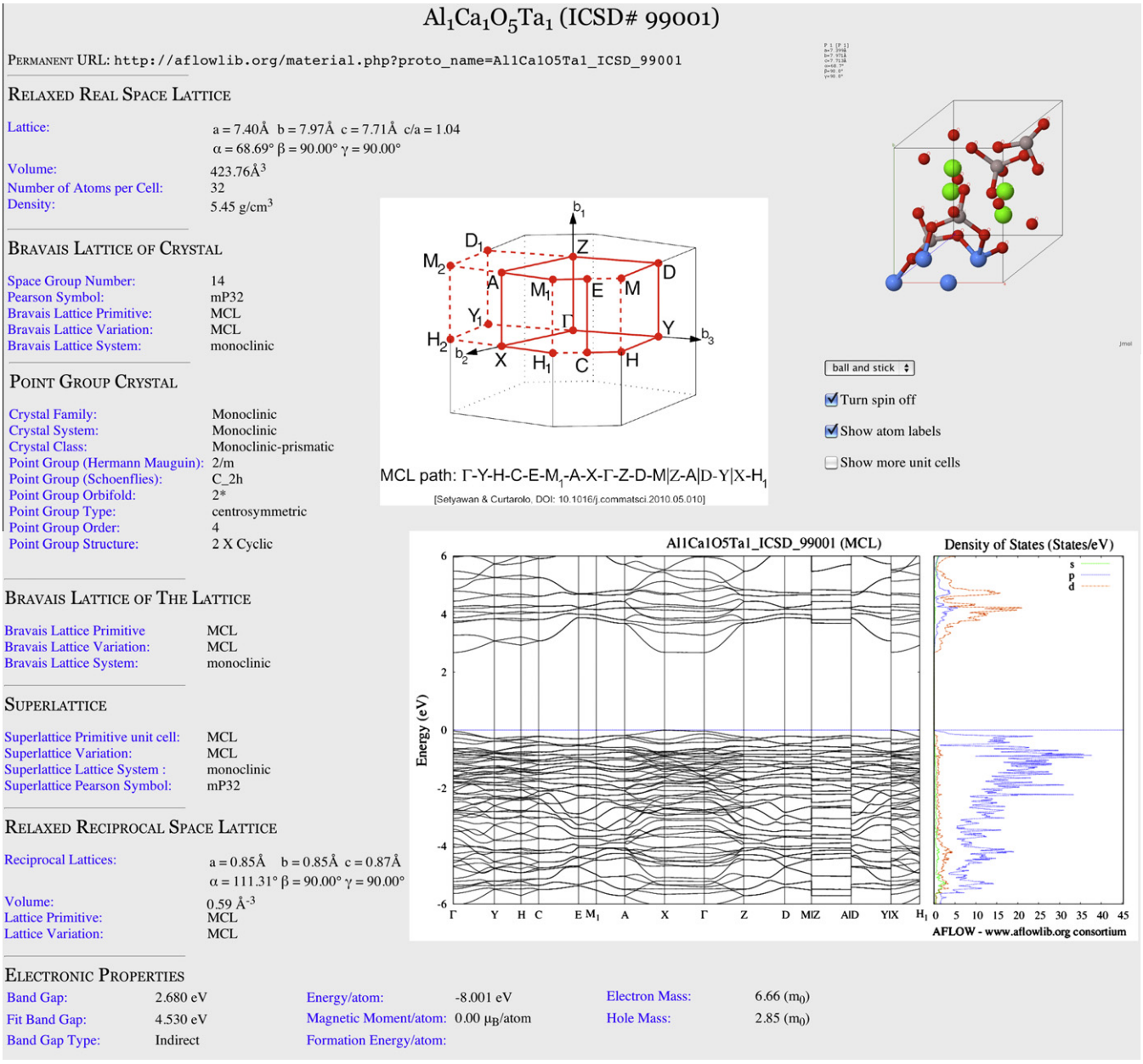

Fig. 10. Example of crystallographic and electronic structure entry in the aflowlib.org database.

- Point Group of the Crystal. This information is important for symmetry characterization. We present the crystal family, system and class, the point group in the Hermann Mauguin and Schönflies notations, the orbifold, point-group central symmetry, its order and its structure. Within AFLOW this information is extracted by the option –edata.
- Bravais Lattice of the Lattice. Bravais Lattice of the (a_1, a_2, a_3) lattice vectors, variation of the Bravais Lattice [25], and lattice system. This information is extracted from the primitive cells when all the atoms are removed (no-basis). Within AFLOW this information is extracted by the option –pgroup.
- Superlattice. If all the atoms are considered of the same species, these items report the Bravais Lattice, its variation, the Lattice system and the Pearson symbol. This information is needed to produce input files for lattice models, such as the cluster expansion.
- Relaxed Reciprocal Space Lattice. Geometry of the reciprocal lattice vectors, volume, Bravais lattice primitive and variation [25].
- Electronic Properties. Band gap (eV), phenomenologically corrected band gap (eV)[23], band gap type (direct or indirect), *ab initio* total energy per atom (eV), magnetic moment per atom (μ_B/atom), *ab initio* formation enthalpy per atom (eV), electron mass at the bottom of the conduction band (m_e), hole mass at the bottom of the valence band (m_h).
- Band Structure (figure). Band structure within the standard **k**-path [25].
- Brillouin Zone (figure). Brillouin Zone with the standard **k**-path [25].
- JMOL Structure (figure). A spinning figure depicting the atoms in a unit cell or supercells.

The information reported in each compound entry is updated regularly as more materials properties are extracted from *ab initio* calculations.

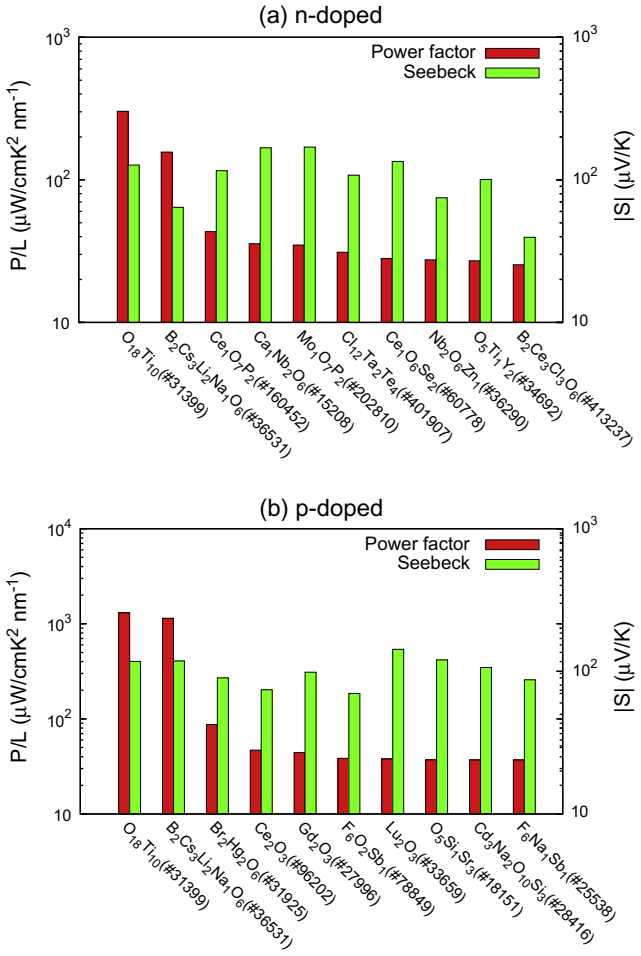

Fig. 11. The best ten (a) *n*- and (b) *p*-doped compounds of highest power factor normalized by grain size. The optimal Seebeck coefficients are shown as well.

4. Example: search for novel nano-grained sintered thermoelectric materials

This database of electronic properties has been used to search for improved nano-grained sintered thermoelectric materials [24]. Thermoelectric devices convert thermal to electric energy, and vice versa, with no moving parts. They are thus highly reliable and portable [26], and are used in a variety of applications, e.g. solid-state refrigerators and energy harvesting devices. However, these applications are limited by the low efficiencies of the currently available commercial thermoelectric compounds [26,27]. Amongst the proposed solutions to overcome this limitation, the sintered nano-powder composites are cost-efficient and have improved efficiency [28]. The grain boundaries in these materials decrease the thermal conductivity κ significantly and hence enhance the thermoelectric performance. In addition to a small κ, a large power factor $P = \sigma^2 S$, with σ the electric conductivity and S the Seebeck coefficient, is required for high efficiency (characterized by the dimensionless thermoelectric figure of merit: $ZT = PT/\kappa$, where T is the temperature). The higher this ZT, the better the performance. A database of thermoelectric properties, as described above, was generated to discover candidate materials with large power factors.

The power factor was calculated using first-principle band structures from the electronic properties database in the constant mean free path approximation [24]. A number of compounds were found that may be promising candidates as nano-structured sintered systems. The ten *n*- and *p*-doped compounds with highest power factor normalized to the grain size in sintered powders are shown in Fig. 11. More details on this study can be found in Ref. [24]. Furthermore, a statistical analysis of the database found correlations between large power factor and band gap, effective carrier masses, and number of atoms in a unit cell without any *a priori* assumptions. These correlations can be used as guidelines for finding better compounds in the future.

5. Challenges and future outlook. The magnetic database

Currently, the production of high-performance magnetic materials depends on the availability of few key elements. Therefore, the search for alternative systems is one of the priorities of the aflowlib.org consortium [29]. We are developing a combinatorial database of potential magnetic materials. Based on a set of appropriate prototypes, we are performing an exhaustive scan of all multi-component configurations. The results are then supplemented with appropriate formation energy calculations to estimate the feasibility of the predicted compounds. Results of this research should be of benefit to the magnetic recording industry as well as to the development of spintronics technology. Furthermore our work may open new avenues to the synthesis on new high performing permanent magnets for energy applications [29].

In Fig. 12, we show the magnetic database search interface. Similarly to the *electronic structure database* it offers the following options:

- Element(s). In this field the user can specify a combination of elements. The syntax is identical to the *electronic structure database*.
- Prototype. In this field the user can restrict the search to particular prototype configurations: *all, $AlCu_2Mn$, $CuLi_2Sn$, etc.*

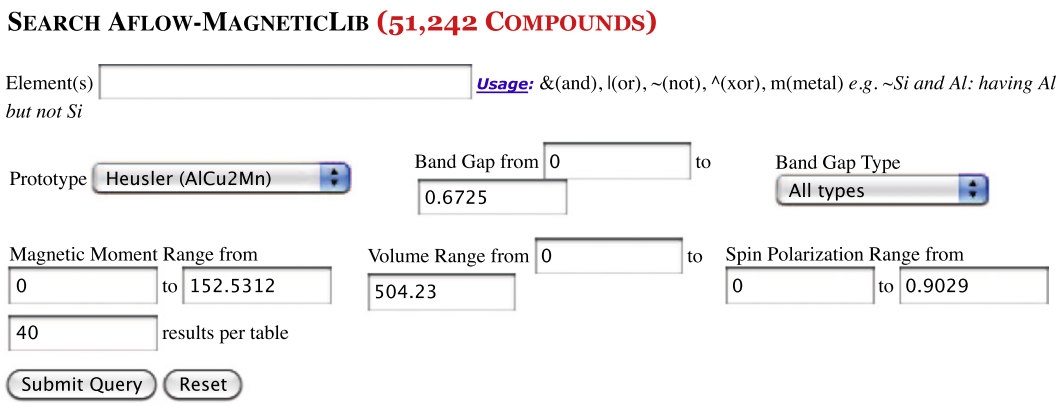

Fig. 12. The interface of the magnetic database currently under development in aflowlib.org.

- Band Gap from/to. In these two fields the search may be restricted to materials with band gap within the specified limits [23].
- Band Gap Type. Provides a choice between *all-types, metals, indirect band gap (I)*, and *direct band gap (D)*.
- Magnetic Moment Range from/to. In these two fields the search can be restricted to materials with a moment/per atom within the specified limits.
- Volume Range from/to. Restrict the search to materials with volume/per cell within the specified limits.
- Spin Polarization Range from/to. In these two fields the user can specify the spin polarization of the density of states at the Fermi level $(N_{up} - N_{down})/(N_{up} + N_{down})$.

The combination of database, keywords and restrictions allow a flexible search of potential compounds. Additional prototypes and options are planned for the near future. A fully functional, consistent and robust magnetic database framework is expected later in 2012.

6. Summary

We describe aflowlib.org, a repository of computational materials databases constructed from HT *ab initio* calculations using the AFLOW framework.

i. The metallic binary alloys database should be helpful to the materials scientist seeking to determine candidate compounds and metastable structures in alloy systems where such information is lacking or controversial.
ii. The electronic structure of inorganic compounds database is being used to uncover new thermoelectric and scintillator materials and should be helpful in screening for additional desirable properties.
iii. The magnetic materials database would be used to search for new materials for magnetic, energy and spintronics applications.

These databases enable data-mining for trends and tendencies that until now have remained hidden due to gaps in the experimental data and to the data scattering associated with variability in the experimental setups and methodologies. They should help overcome some of the obstacles associated with carrying out costly and difficult experimental studies. All the data is available in the online repository, aflowlib.org.

Acknowledgments

The authors acknowledge Gerbrand Ceder, Dane Morgan, Leeor Kronik, and Bobby Sumpter for fruitful discussions. Research supported by ONR (N00014-11-1-0136, N00014-10-1-0436, N00014-09-1-0921), NSF (DMR-0639822, DMR-0908753), and the Department of Homeland Security – Domestic Nuclear Detection Office. SC acknowledges support by the Feinberg fellowship at the Weizmann Institute of Science. MBN wishes to acknowledge partial support from the Office of Basic Energy Sciences, DOE at Oak Ridge National Laboratory under contract DE-AC05-00OR22725 with UT-Battelle, LLC. SS wishes to thank Science foundation of Ireland (07/IN.1/I945) and CRANN for financial support. Computational resources provided by Fulton Supercomputer Center at Brigham Young University, Teragrid (MCA-07S005), Trinity Center for High Performance Computing, Center for Nanophase Materials Sciences (CNMS2010-206), and the National Center for Computational Sciences at Oak Ridge National Laboratory.

References

[1] P.S. White, J.R. Rodgers, Y.L. Page, Acta Cryst. B 58 (2002) 343.
[2] A. Belsky, M. Hellenbrandt, V.L. Karen, P. Luksch, Acta Cryst. B58 (2002) 364–369.
[3] P. Villars, L. Calvert, Pearson's Handbook of Crystallographic Data for Intermetallic Phases, 2nd ed., ASM International, Materials Park, OH, 1991.
[4] P. Villars, K. Cenzual, J.L.C. Daams, F. Hulliger, T.B. Massalski, H. Okamoto, K. Osaki, A. Prince, S. Iwata, Crystal Impact, Pauling File. Inorganic Materials Database and Design System, Binaries ed., ASM International, Metal Park, OH, 2003.
[5] T.B. Massalski, H. Okamoto, P.R. Subramanian, L. Kacprzak (Eds.), Binary Alloy Phase Diagrams, American Society for Metals, Materials Park, OH, 1990.
[6] P. Villars, M. Berndt, K. Brandenburg, K. Cenzual, J. Daams, F. Hulliger, T. Massalski, H. Okamoto, K. Osaki, A. Prince, H. Putz, S. Iwata, J. Alloys Comp. 367 (2004) 293–297.
[7] P. Villars, K. Brandenburg, M. Berndt, S. LeClair, A. Jackson, Y.H. Pao, B. Igelnik, M. Oxley, B. Bakshi, P. Chen, S. Iwata, J. Alloys Comp. 317–318 (2001) 26–38.
[8] S. Curtarolo, W. Setyawan, G.L.W. Hart, M. Jahnatek, R.V. Chepulskii, R.H. Taylor, S. Wang, J. Xue, K. Yang, O. Levy, M. Mehl, H.T. Stokes, D.O. Demchenko, D. Morgan, AFLOW: An Automatic Framework for High-throughput Materials Discovery, Comput. Mater. Sci. (2012), doi:10.1016/j.commatsci.2012.02.005.
[9] A. Jain, G. Hautier, C.J. Moore, S.P. Ong, C.C. Fischer, T. Mueller, K.A. Persson, G. Ceder, Comput. Mater. Sci. 50 (2011) 2295–2310.
[10] D. de Fontaine, Cluster approach to order-disorder transformations in alloys, Solid State Physics, vol. 47, Academic Press, New York, 1994.
[11] R.H. Taylor, S. Curtarolo, G.L.W. Hart, Phys. Rev. B 84 (2011) 084101.
[12] O. Levy, R.V. Chepulskii, G.L.W. Hart, S. Curtarolo, J. Am. Chem. Soc. 132 (2010) 833.
[13] O. Levy, M. Jahnatek, R.V. Chepulskii, G.L.W. Hart, S. Curtarolo, J. Am. Chem. Soc. 133 (2011) 158–163.
[14] M. Jahnatek, O. Levy, G.L.W. Hart, L.J. Nelson, R.V. Chepulskii, J. Xue, S. Curtarolo, Phys. Rev. B 84 (2011) 214110.
[15] A.R. Harutyunyan, N. Awasthi, A. Jiang, W. Setyawan, E. Mora, T. Tokune, K. Bolton, S. Curtarolo, Phys. Rev. Lett. 100 (2008) 195502.
[16] S. Curtarolo, N. Awasthi, W. Setyawan, A. Jiang, K. Bolton, T. Tokune, A.R. Harutyunyan, Phys. Rev. B 78 (2008) 054105.
[17] R.V. Chepulskii, S. Curtarolo, ACS Nano 5 (2011) 247–254.
[18] S. Curtarolo, D. Morgan, G. Ceder, Calphad 29 (2005) 163.
[19] O. Levy, G.L.W. Hart, S. Curtarolo, Acta Mater. 58 (2010) 2887–2897.
[20] O. Levy, J. Xue, S. Wang, G.L.W. Hart, S. Curtarolo, Phys. Rev. B 85 (2012) 012201.
[21] O. Levy, G.L.W. Hart, S. Curtarolo, Phys. Rev. B 81 (2010) 174106.
[22] A.D. Mighell, V.L. Karen, Acta Cryst. A49 (1993) c409.
[23] W. Setyawan, R.M. Gaume, S. Lam, R.S. Feigelson, S. Curtarolo, ACS Combust. Sci. 13 (2011) 382–390.
[24] S. Wang, Z. Wang, W. Setyawan, N. Mingo, S. Curtarolo, Phys. Rev. X 1 (2011) 021012.
[25] W. Setyawan, S. Curtarolo, Comput. Mater. Sci. 49 (2010) 299.
[26] G.S. Nolas, J. Sharp, H.J. Goldsmid, Thermoelectrics: Basic Principles and New Materials Developments, Springer-Verlag, 2001.
[27] C.B. Vining, Nat. Mater. 8 (2009) 83–85.
[28] G. Joshi, H. Lee, Y. Lan, X. Wang, G. Zhu, D. Wang, R.W. Gould, D.C. Cuff, M.Y. Tang, M.S. Dresselhaus, G. Chen, Z. Ren, Nano Lett. 8 (2008) 4670–4674.
[29] N. Jones, Nature 472 (2011) 22–23.